Journal of Molecular Neuroscience (2019) 67:48–61
https://doi.org/10.1007/s12031-018-1209-9

Unrestricted Somatic Stem Cells Loaded in Nanofibrous Conduit as Potential Candidate for Sciatic Nerve Regeneration

Saeed Farzamfar[1] · Arian Ehterami[2] · Majid Salehi[3,4] · Ahmad Vaeez[1] · Amir Atashi[4,5] · Hamed Sahrapeyma[6]

Received: 8 August 2018 / Accepted: 8 November 2018 / Published online: 27 November 2018

Abstract

Motor and sensory recovery following critical size peripheral nerve defects is often incomplete. Although nerve grafting has been proposed as the gold standard, it is associated with several disadvantages. Here we report a novel approach to peripheral nerve repair using Human Unrestricted Somatic Stem Cells (USSC) delivered through an electrospun neural guidance conduit. Conduits were produced from PCL and gelatin blend. Several in vitro methods were utilized to investigate the conduit's physicochemical and biological characteristics. Nerve regeneration was studied across a 10-mm sciatic nerve gap in Wistar rats. For functional analysis, the conduits were seeded with 3×10^4 USSCs and implanted into a 10-mm sciatic nerve defect. After 14 weeks, the results of functional recovery analysis and histopathological examinations showed that animals implanted with USSC containing conduits exhibited improved functional and histopathological recovery which was more close to the autograft group compared to other groups. Our results support the potential applicability of USSCs to treat peripheral nerve injury in the clinic.

Keywords Unrestricted somatic stem cells · Neural guidance conduits · Electrospinning · Peripheral nerve regeneration

Introduction

Peripheral nerve injuries cause pain and significant disability in many affected patients (Miller et al. 2016). For peripheral nerve damages that result in critical size defects, nerve grafting is performed as the gold standard of treatment. However, this treatment option has several disadvantages such as limited harvestable nerve, the donor site damage, and the necessity for multiple surgeries (Gao et al. 2016). Allograft is another treatment modality; however, the risk of transmittable diseases and immune rejection are unsolved issues (Kehoe et al. 2012). Therefore, alternative strategies are highly demanded.

One of the potential strategies to improve peripheral nerve repair, cell-based therapy represents a promising tool for regenerating the defective nerve tissue (di Summa et al. 2010; Kemp et al. 2008). Among various cell types, Schwan

Saeed Farzamfar, Arian Ehterami and Majid Salehi contributed equally to this work.

✉ Majid Salehi
salehi.m@shmu.ac.ir

Saeed Farzamfar
farzamfar.saeed@gmail.com

Arian Ehterami
arian.ehterami@srbiau.ac.ir

Ahmad Vaeez
ahmadvaez@yahoo.com

Amir Atashi
atashia@shmu.ac.ir

Hamed Sahrapeyma
hamed.sahrapeyma@yahoo.com

[1] Department of Tissue Engineering and Applied Cell Sciences, School of Advanced Technologies in Medicine, Tehran University of Medical Sciences, Tehran, Iran

[2] Department of Mechanical and Aerospace Engineering, Science and Research Branch, Islamic Azad University, Tehran, Iran

[3] Department of Tissue Engineering, School of Medicine, Shahroud University of Medical Sciences, Shahroud, Iran

[4] Tissue Engineering and Stem Cells Research Center, Shahroud University of Medical Sciences, Shahroud, Iran

[5] Department of Hematology, School of Medicine, Shahroud University of Medical Sciences, Shahroud, Iran

[6] Department of Biomedical Engineering, Science and Research Branch, Islamic Azad University, Tehran, Iran

cells (SCs) have shown the most effectiveness to treat peripheral nerve injuries. However, their isolation and expansion are associated with several disadvantages such as the sacrifice of a donor nerve, donor site morbidity, and unavailability of a harvestable tissue (Jessen and Mirsky 2016; Sanen et al. 2017; Sparling et al. 2015). These problems have driven efforts to search for alternative supporting cells in the field of peripheral nerve regenerative medicine.

Stem cell therapy has established itself as a promising field of regenerative medicine (Murakami et al. 2016). While the bone marrow-derived stem cells lead the researches, other sources of stem cells have been investigated, seeking sources with higher potential (Polymeri et al. 2016; Marín 2016). Currently, there is a growing interest in the clinical potential of stem cells isolated from disposable tissues such as the amniotic fluid, placenta, and umbilical cord blood (Fauza and Bani 2016; Mimeault et al. 2007). Human unrestricted somatic stem cells (USSCs) represent a novel source of stem cells which are recognized by their remarkable proliferative capacity, ease of harvest, and lack of ethical dilemmas (Ghodsizad et al. 2009). Secretion of neurotrophic factors, neural differentiation potential, and immunomodulatory activities are their possible footholds as therapeutic agents for peripheral nerve regeneration (Santourlidis et al. 2011; Schwartz et al. 2008; Nauta and Fibbe 2007).

The use of a suitable cell delivery vehicle in the peripheral nerve injury site may enhance stem cells potential in the healing process (Ma et al. 2017; Faroni et al. 2015). Use of neural guidance conduits (NGCs) made of synthetic and/or natural polymers provides a suitable platform for cell delivery (Muheremu and Ao 2015). For the development of next generation of NGCs, great efforts have been dedicated to mimicking the structures and components of the autologous nerves (Tung et al. 2015; Jiang et al. 2014). With the progress of fabrication methods, structures of NGCs have been greatly improved to meet different requirements including porous channel wall allowing for good nutrients diffusion along with suitable mechanical properties to prevent rupture during suturing process (Jiang et al. 2014; de Ruiter et al. 2009). In addition, with the increasing understanding of cell-material interactions, more attention is directed towards the fabrication of scaffolds that can mimic the structural and componential features of extracellular matrix (ECM) to stimulate desirable cellular activities such as cell attachment, cell proliferation, and cell differentiation (Sill and von Recum 2008; Lannutti et al. 2007).

ECM of tissues is composed of a three-dimensional (3-D) network of 50–500 nm diameter structural protein and polysaccharide fibers (Alberts et al. 2002). Electrospinning is a method of fabrication of nanofibrous scaffolds which highly resemble the structural hierarchy of natural ECM (Li et al. 2006). Electrospun nanofibrous scaffolds offer a high surface area for better cell adhesion and possibly topographical cues for directing cellular functions (Peng et al. 2016). These unique characteristics have made them appealing for neural tissue engineering (Cao et al. 2009).

Cellular behavior on the scaffolds greatly depends on the characteristics of the polymer or polymers used in the fabrication of matrices (Barnes et al. 2007). In general, using a single polymer cannot meet all the requirements of an ideal scaffold, but by taking polymer blends or copolymers, it is possible to attain a scaffold with desired properties (Lee et al. 2012; Bhattarai et al. 2009). PCL is a synthetic aliphatic polyester that shows a high mechanical strength, biocompatibility, and biodegradability (Kweon et al. 2003). Although the scaffolds composed of PCL nanofibers architecturally imitate the natural ECM, lack of cell recognition sites and poor hydrophilicity hurdle their tissue engineering applications (Sarasam and Madihally 2005). On the other hand, gelatin is a natural material which is derived from collagen by controlled hydrolysis (Parenteau-Bareil et al. 2010). Because of its many merits such as biodegradability, biocompatibility, and low-cost, gelatin has gained attention in biomedical applications (Hoque et al. 2015). However, this polymer fails to impart the required mechanical strength to produced scaffolds (Huang et al. 2004; Meng et al. 2010). Preliminary studies have indicated that combination of PCL and gelatin can solve the drawbacks associated with natural and synthetic polymers, exploiting the advantages of each one which results in a new biomaterial with improved physical and biological properties (Zhang et al. 2005; Ghasemi-Mobarakeh et al. 2008). In the present study, we fabricated the PCL/gelatin NGCs using the electrospinning method and then seeded them with USSCs to improve their healing potential. Physicochemical and biological properties of fabricated NGCs were studied using various in vitro methods. Furthermore, we examined the level of nerve repair in a critical size defect in rats using several functional analyzing methods, electrophysiological tests, and histopathological evaluations of the muscle and nerve tissues.

Materials and Methods

Fabrication and Characterization of Electrospun PCL/Gelatin Nerve Conduits

Firstly, PCL (average Mn 80,000 (CAS Number: 24980-41-4, Aldrich)) was dissolved in acetic acid (CAS Number: 64-19-7, Aldrich) to the final concentration of 14 *w*/*v* %. Similarly, gelatin (CAS Number: 9000-70-8, Aldrich) solution (14 *w*/*v* %) was prepared in acetic acid at room temperature. Then PCL and gelatin solutions were mixed at the volume ratio of 70:30 (PCL/gelatin) and stirred for 24 h. The resulting solution was transferred to a 10-mL syringe ending to an 18-gauge metal needle and the syringe was placed in a syringe pump (SP1000, Fanavaran Nano-Meghyas, Iran) with 15 cm

distance between the needle tip and the collecting mandrel. A positive high voltage (20 kV) was applied to the needle tip and the flow rate was set to 0.5 mL/h. The NGC with the size of 14 mm and the inner diameter of about 1 mm was prepared by rolling up the PCL/gelatin electrospun sheets (Fig. 1a). NGCs were then cross linked in a 1% (wt/v) glutaraldehyde (CAS Number: 111-30-8, Aldrich) solution in ethanol for 6 h followed by washing in 0.1 M glycine aqueous solution for 30 min and then in distilled water three times.

Scanning Electron Microscopy Analysis of Scaffolds

The morphology of the PCL/gelatin scaffolds was studied by scanning electron microscope (SEM; DSM 960A, Zeiss, Germany) at 15 kV by coating with gold for 250 s using a sputter coater (SCD 004, Balzers, Germany).

Contact Angle Measurement

The hydrophilicity of the PCL/gelatin and PCL-only substrates was investigated using a static contact angle measuring device (KRUSS, Hamburg, Germany).

Weight Loss Measurement

For in vitro degradation rate measurement, the PCL/gelatin and PCL-only scaffolds were weighted, and totally immersed in 10 mL of PBS and kept at 37 °C in an incubator. After predetermined degradation times (30 and 60 days), samples were taken out and dried to a constant weight. Weight loss was calculated using the Eq. 1 as we previously described (Salehi et al. 2015).

Where "$W0$" is the initial weight of samples and "$W1$" is the dry weight after removing from the media.

$$\text{Weight loss}\ (\%) = \frac{W0 - W1}{W0} \times 100 \tag{1}$$

Mechanical Properties (Tensile Strength and Young's Modulus)

Mechanical analysis (tensile strength and Young's modulus) was carried out on PCL/gelatin and PCL-only scaffolds (80 mm × 10 mm) by an Instron 5566 universal testing machine (Instron, USA) at a strain rate of 10 mm/min.

Porosity Measurement

To evaluate the porosity of the scaffolds, liquid displacement method was exploited using the Eq. 2:

$$\text{Porosity}\ (\%) = \frac{V_1 - V_3}{V_2 - V_3} \times 100 \tag{2}$$

Where V_1 is initial volume of 96% ethanol, V_2 is its volume after scaffold immersion, and V_3 is the volume of the ethanol after the scaffold removal.

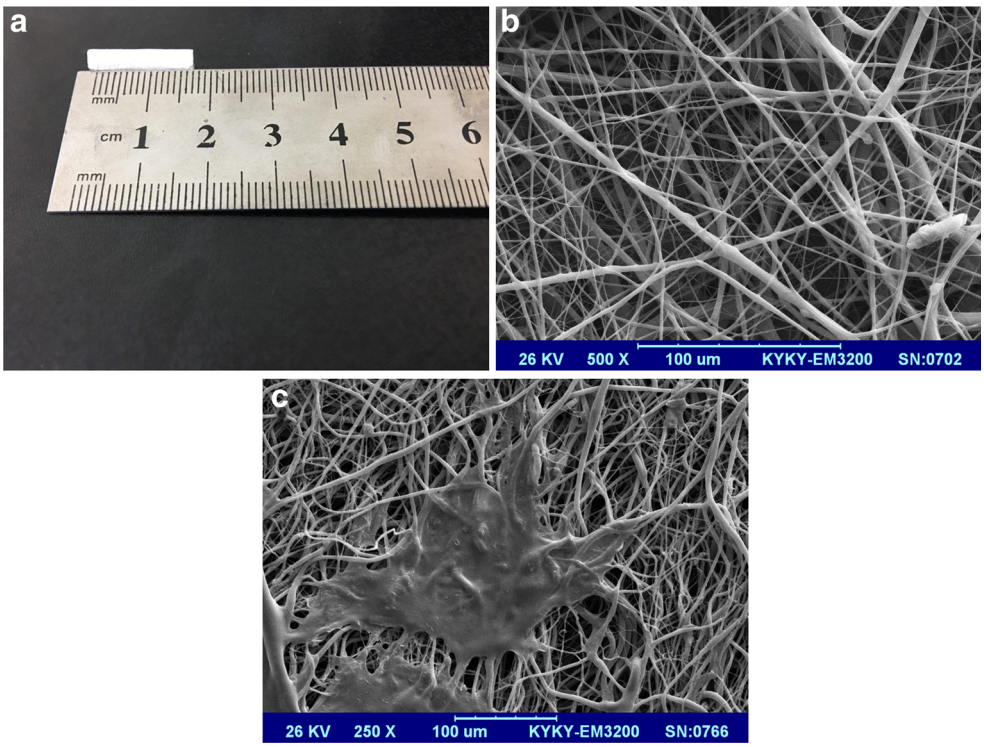

Fig. 1 **a** Photomacrograph of the conduits produced from electrospun matrices, **b** representative SEM images of the PCL/gelatin electrospun yarns, and **c** representative SEM images of Schwann cells cultured on electrospun PCL/gelatin nanofibrous scaffolds

Schwann Cells Isolation

SCs were isolated from the sciatic nerves of adult male Wistar rats (weighing 200–250 g) according to our previous study (Hoque et al. 2015). The cells were cultivated in Dulbecco's modified Eagle's medium: nutrient mixture F-12 (DMEM/F12; Gibco, Grand Island) supplemented with 10% (*v*/*v*) fetal bovine serum (FBS; Gibco, Grand Island), 100 unit/mL of penicillin, and 100 μg/mL of streptomycin in a humidified incubator at 37 °C with 5% CO_2.

Cell Viability Assay

The viability of SCs grown on the PCL/gelatin and PCL-only scaffolds was evaluated by using 3-(4,5-dimethyl thiazol-2-yl)-2,5-diphenyl tetrazolium bromide (MTT) assay after 1, 3, 7 days of cell seeding. Scaffolds were cut into appropriate sizes and placed in each well of 96-well plates and seeded with SCs at the density of 1×10^4 cells per scaffold. At each time interval, the culture medium in the wells was aspirated and 200 μL of 0.5 mg/mL MTT solution was added to each well and incubated for 4 h. After the incubation period, the MTT solution was discarded, and after the formazan crystals had formed, they were dissolved in 150 μL DMSO and the plate was incubated in a dark place for 10 min on a rotary shaker. The absorbance values of the samples were read at 570 nm by an ELISA reader (Expert 96, Asys Hitch, Ec Austria).

Cell Adhesion and Morphology Studies

Of SCs, 1×10^4 were seeded onto PCL/gelatin scaffolds and cultured for 24 h. After this time period, the cell-scaffold constructs were rinsed with PBS and then fixed in 4% glutaraldehyde solution at ambient conditions for 2 h. The samples were then dehydrated via graded concentrations of ethanol in distilled water. The samples were dried and after sputter coating observed under the SEM. 4′,6-Diamidino-2-phenylindole (DAPI) staining was used to further evaluate the cell attachment. After 2 days of incubation, SCs grown on electrospun scaffolds were rinsed twice with PBS. The cells were fixed with fresh 3.7% paraformaldehyde in PBS for 10 min. Then the samples were washed with PBS and permeabilized with 0.1% Triton X-100 (in PBS) for 5 min. DAPI staining solution (1:1000 dilution) was added onto the scaffolds and incubated in dark for 20 min. The SCs attached on the scaffolds were examined under the fluorescent microscope, after repeated washing with PBS.

USSCs Isolation and Culture

Harvest and culture of human USSCs were carried out as described previously by Kogler et al. (Kögler et al. 2004). Informed consent was obtained from all parents before blood collection. Umbilical cord vein blood was collected and its mononuclear cell fraction was separated by Ficoll-Hypaque density gradient centrifugation. USSCs were cultured in low-glucose Dulbecco's Modified Eagle's Medium supplemented with 30% fetal calf serum (FCS), dexamethasone (10^{-7} M), penicillin (100 units/mL), streptomycin (100 μg/mL), and ultraglutamine (2 mM). Cells were incubated in a humidified incubator with 95% air and 5% CO_2 at 37 °C. After the incubation period, when USSC reached 80% confluency, they were detached by 0.25% trypsin treatment and passaged.

Osteogenic and Adipogenic Differentiation

Osteogenic and adipogenic differentiation of USSCs was performed according to a protocol as we previously described (Ahmadbeigi et al. 2010). For osteogenic differentiation, the cells were grown in culture medium containing 10^{-8} M dexamethasone, 0.2 mM ascorbic acid 2-phosphate, and 10 mM β-glycerophosphate. The medium was refreshed every 3 days. After 21 days of culture, the presence of hydroxyapatite crystals was evaluated by Alizarin Red (Sigma–Aldrich) staining according to the manufacturer's instructions. For adipogenic differentiation, the cells were grown in induction media containing 0.5 mM hydrocortisone, 0.5 mM isobutylmethylxanthine, and 60 mM indomethacin. After 3 weeks of culture, Oil Red O staining (Sigma–Aldrich) was performed according to the protocol provided by the manufacturer to confirm differentiation to this lineage.

Flow Cytometry

USSCs were characterized by flow cytometry for the expression of surface markers using mouse monoclonal antibodies against human CD34, CD45, CD73, CD105, and CD166 (all from eBioscience). Cells were incubated with each antibody according to the manufacturer's instructions for 1 h and then studied by Attune flow cytometry (Applied Biosystems) and FlowJo software.

In Vivo Studies

Sciatic Nerve Defect

Thirty healthy adult male Wistar rats (3 months old, weighing 250–270 g) were purchased from Pasture Institute (Tehran, Iran). Animal experiments were approved by the ethics committee of Shahroud University of Medical Sciences and were performed in accordance with the university guidelines. The rats were randomly divided into five groups: (1) Positive control (rats without sciatic nerve injury), (2) Negative control (with nerve injury but without surgical interventions), (3) Autograft, (4) NGCs without cells, (5) NGCs seeded with

USSCs (3×10^4 cells in each conduit). For sciatic nerve defect model creation, the animals were anesthetized by intraperitoneal injection of ketamine 5%/xylazine 2% (25% (*v*/*v*), 0.10 mL/100 g body weight). Their right lower limb's skin was shaved and disinfected by povidone-iodine. After skin incision, a 10-mm-long segment of their sciatic nerve was resected. For the rats in the NGC and NGC/USSCs group, 2 mm of distal and proximal nerve stumps was inserted into the conduit's lumen and their epineurium was sutured to the conduit's wall by no. 6-0 polyglycolic acid suture (SUPA Medical Devices, Tehran, Iran) leaving a 10-mm gap between two ends. Nerve gap in the autograft group was bridged by resected nerve segment, which was reversed and sutured to the proximal and distal nerve stumps.

Walking-Foot-Print Analysis

Sciatic functional index (SFI) was evaluated by recording the rats' footprints 4 and 8 weeks post-surgery. At each time interval, rat's hind paws were painted with ink and they were left to walk through an acrylic corridor (43 cm length, 8.70 cm width, and 5.50 cm height) ended to a darkened goal box. White papers covered the floor of the corridor to record the foot printings. The SFI was calculated according to a method as we described previously (Farzamfar et al. 2018). SFI = 0 represented the normal function, while the SFI = − 100 represented the complete loss of function.

Functional Assessment of Sensory Recovery (Hot Plate Test)

Fourteen weeks post-surgery, rats were investigated for thermal pain sensitivity by placing their injured limb on a hot plate (56 °C). The time passed on the hot plate until the animals reacted by licking their paws or jumping was recorded. The cutoff time for their reaction was set at 12 s.

Nerve Conduction Test

Fourteen weeks after surgery, compound muscle action potential (CMAP) amplitudes of the sciatic nerves were recorded. The animals were anesthetized by intraperitoneal injection of ketamine 100 mg/xylazine 10 mg/kg body weight. The skin was shaved and the sciatic nerve was exposed. Sciatic nerve just before the injury site was stimulated with an electric stimulus (3–5 mA) using a needle electrode. The CMAP amplitudes were measured from the needle and the response of the gastrocnemius muscle was recorded by the cap electrodes located on it (filtering frequency of 10 Hz to 10 kHz, sensitivity of 2 mV/division, and sweep speed of 1 ms/division,) using an electromyographic recorder (Negarandishegan, Tehran, Iran).

Gastrocnemius Muscle Wet Weight Loss

At the end of 14th-week post-surgery, rats were sacrificed and the posterior gastrocnemius muscles on the operated and non-operated hind limbs were harvested and their weight was immediately measured to calculate the wet weight loss of gastrocnemius muscles using the Eq. 3.

$$\text{Gastrocnemius muscle wet weight loss } (\%) = \left(1 - \frac{\text{Wet weight of the muscle on the injured side}}{\text{Wet weight of the muscle on the uninjured side}}\right) \times 100 \quad (3)$$

Histopathological Examination

At the end of 14th-week post-surgery, the animals were sacrificed and their sciatic nerve and gastrocnemius muscle were harvested and fixed in a 10% buffered formalin. After processing and embedding in paraffin, they were sectioned into 5 μm sizes and stained with hematoxylin-eosin (H&E). The prepared tissue slides were observed and imaged under a light microscope (Carl Zeiss, Thornwood) with a digital camera (Olympus, Tokyo, Japan).

Statistical Analysis

The results were statistically analyzed by Graph pad prism version 5 software using one-way ANOVA and post hoc test. The data were expressed as the mean ± standard deviation (SD). All experiments were performed at least three times and in all evaluations, $p < 0.05$ was considered as the statistically significant.

Results

Scaffold Characterization

Figure 1a, b illustrates the macroscopic and microscopic images of the scaffolds, respectively. SEM observation revealed that the scaffolds were composed of randomly oriented fibers with diameters of about 856 ± 69 nm. This ECM-like structure may be favorable to improve axonal outgrowth and extension (Xie et al. 2014; Xie et al. 2010). Surface wettability is an important feature of the scaffolds which can affect the attachment, proliferation, migration, and viability of cells (Fu et al. 2014). The results of surface wettability measurement (Table 1) showed that PCL scaffolds had the highest contact angle (111.8 ± 7.6°) which is consistent with its hydrophobic nature (Tran et al. 2015). The incorporation of gelatin with PCL significantly reduced the contact angle to 66.4 ± 8.1° (p value < 0.005) making it more favorable for cellular activities (Naseri-Nosar et al. 2017). An ideal NGC should be

Table 1 Characterization of the scaffolds. Values represent the mean ± SD, $n = 4$, $^{*}p < 0.05$, $^{**}p < 0.01$, and $^{***}p < 0.005$

Samples	Contact angle (°)	Mechanical strength (MPa)	Porosity (%)	Weight loss after 30 days (%)	Weight loss after 60 days (%)
PCL	111.8 ± 7.6***	4.86 ± 0.07*	78.6 ± 4.5	1.83 ± 0.34	9.10 ± 1.47
PCL/gelatin	66.4 ± 8.1	2.83 ± 0.44	76.7 ± 3.2	47.16 ± 3.97***	72.46 ± 2.57***

biodegradable to obviate extra surgery for conduit removal after regeneration (Salehi et al. 2017). Table 1 shows the weight loss percentage of NGCs in phosphate-buffered saline solution after 30 and 60 days. Results showed that PCL's weight loss percentage was negligible after 30 days (1.83 ± 0.34%). Incorporation of gelatin with PCL significantly increased the degradation rate of the scaffolds at both time intervals (p value < 0.005). This can be due to the higher hydrophilicity of PCL/gelatin scaffolds and consequently further interaction with water molecules (Binulal et al. 2014). NGCs require a good mechanical strength to withstand suturing and to prevent collapse when implanted (Salehi et al. 2017). The analysis of mechanical properties (Table 1) showed that PCL scaffolds had a significantly higher tensile strength compared to PCL/gelatin samples (4.86 ± 0.07 vs. 2.83 ± 0.44 MPa). This can be due to the superior mechanical strength of PCL compared to gelatin (Yao et al. 2016). The mechanical properties have a direct influence on suturing ability, and the higher the ultimate tensile strength, the easier the suturing during grafting surgery (Naseri-Nosar et al. 2017). We could show that the ultimate tensile strength values measured for all NGCs were greater than that of the fresh transected adult rat sciatic nerve (0.78 MPa) (Wang et al. 2009). The suitable porosity of the NGC's wall facilitates nutrients diffusion through the conduit and enhances nerve regeneration (de Ruiter et al. 2009). The results of porosity measurement (Table 1) showed that PCL and PCL/gelatin conduits had an average porosity of 78.6 ± 4.5 and 76.7 ± 3.2%, respectively. Statistically, no significant difference was observed between the two measurements. It is generally accepted that the optimum porosity percentage for a suitable tissue engineered scaffold is above 80% (Ghasemi-Mobarakeh et al. 2007). Therefore, the fabrication method utilized in this study could not produce scaffolds with ideal porosity.

In Vitro Biological Evaluations of the NGCs

Cell Viability and Proliferation Assay

SCs play a major role to support the repair of injured peripheral nerves (Jessen and Mirsky 2016). A significant body of studies has implanted SCs with NGCs to enhance nerve regeneration (Jessen et al. 2015; Luo et al. 2015; Fairbairn et al. 2015). Hence, NGCs with a beneficial effect on the SCs is desirable in peripheral nerve tissue engineering. MTT assay was conducted to investigate the effects of nanofibrous scaffolds on the proliferation and viability of SCs. As shown in Fig. 2, during 7 days of culture, SCs went through a considerable increase on PCL/gelatin scaffolds indicating that these scaffolds can support the proliferation of SCs. At 7 days the amount of SCs on PCL/gelatin scaffolds surpassed that on tissue culture plate and PCL scaffolds. The higher absorbance values in PCL/gelatin group compared to PCL group can be due to the presence of gelatin which is known to have excellent cell adhesion and proliferative properties (Gautam et al. 2013).

Cell Attachment Analysis on the NGCs

Cell adhesion is an important parameter which markedly influences various cellular responses including proliferation and migration within the scaffold as well as tissue repair time (Chang and Wang 2011). To investigate the cell attachment to the scaffolds, the presence of SCs in fabricated films was investigated using DAPI staining and SEM. Figure 1c illustrates the SEM images of SCs grown on electrospun PCL/gelatin scaffolds. It is clear that SCs could show good attachment on the nanofibrous scaffolds. The results of DAPI staining (Fig. 3) showed that the number of cells attaching to the PCL/gelatin scaffolds was greater than those present on PCL-only samples. This is not surprising because the presence of gelatin enhances cell attachment due to its numerous cell

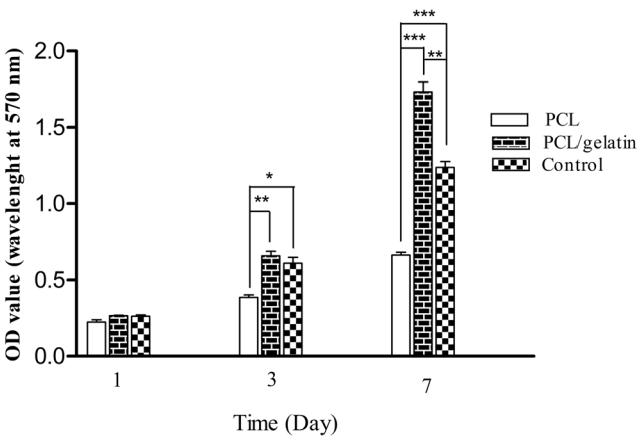

Fig. 2 Histogram comparing the viability of Schwann cells on the PCL and PCL/gelatin scaffolds obtained by MTT assay 1, 3, and 7 days after cell seeding. Values represent the mean ± SD, $n = 3$, $^{*}p < 0.05$, $^{**}p < 0.01$, and $^{***}p < 0.005$

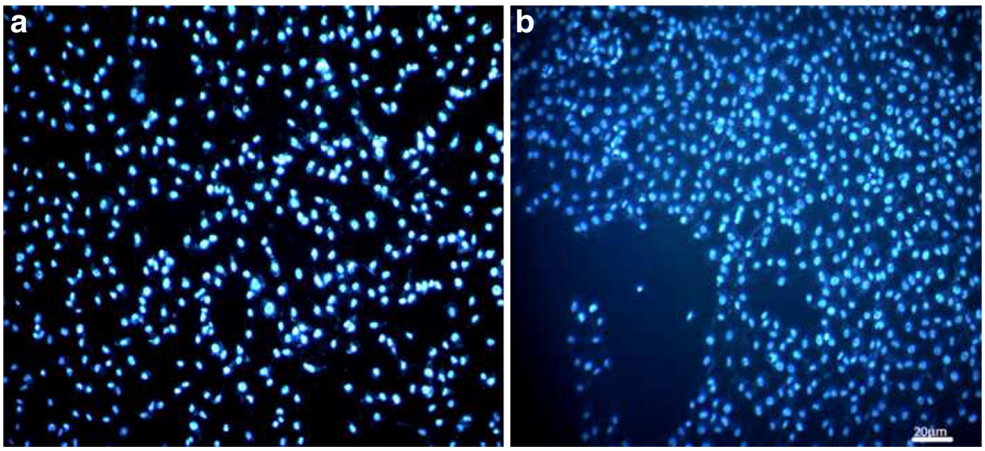

Fig. 3 DAPI staining images of Schwann cells on PCL and PCL/gelatin scaffolds. **a** For PCL and **b** for PCL/gelatin scaffolds

adhesion sites while high hydrophobicity of PCL hampers cell attachment to the PCL-only substrates (Ghasemi-Mobarakeh et al. 2008; Liu et al. 2009). These results indicated that PCL/gelatin matrices were more conducive to cell attachment and proliferation.

USSC Characterization

USSCs demonstrated fibroblast-like morphology which could adhere to the tissue culture plate (Fig. 4a). The results of the flow cytometry study showed that USSCs were positive for CD73, CD105, and CD166 but were negative for CD34 and CD45 (Fig. 5). Furthermore, adipogenic and osteogenic differentiation potential of USSCs was validated by Oil Red O and Alizarine Red S staining, respectively (Fig. 4b, c).

In Vivo Regenerative Capacity of Conduits

Sciatic Function Index

For motor function recovery study, walking track analysis is often performed in the rat model of sciatic nerve injury (Lee et al. 2013). Figure 6 displays the average SFI values for all groups. The negative control group showed a slight improvement from -92.23 ± 6.40 after 4th week to -85.067 ± 3.69 at the end of 8th week post-surgery. The autograft as the gold

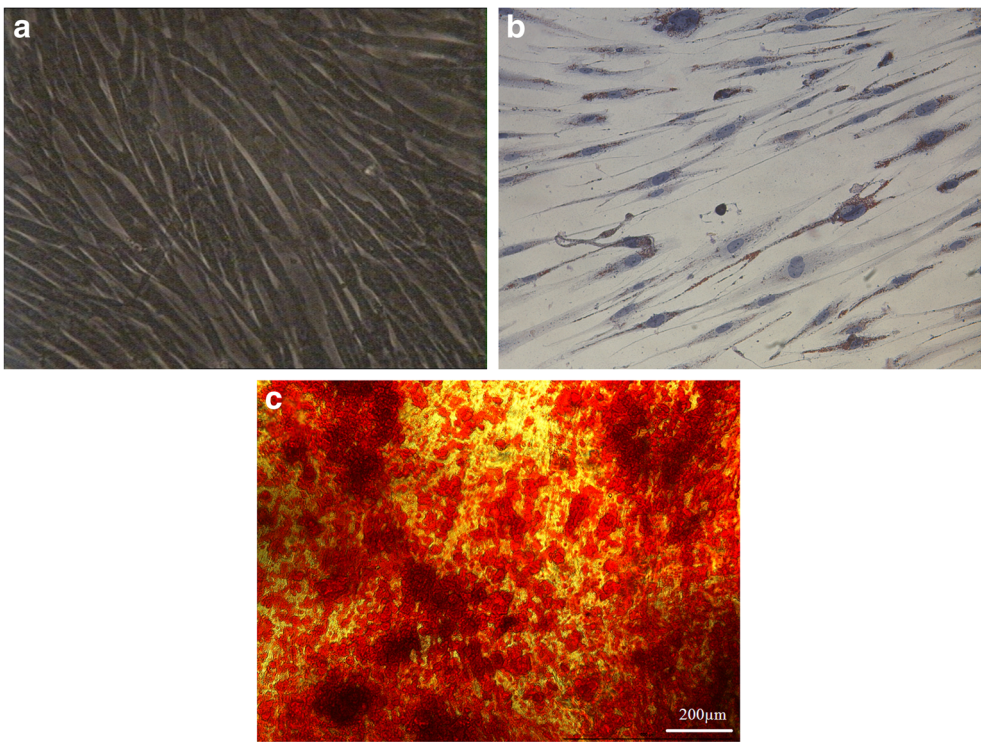

Fig. 4 **a** Representative live microscopy images (objective magnification ×400) of USSCs, **b** Oil Red O staining images of USSCs (objective magnification ×100) after 3 weeks of culture under adipogenic differentiation medium, and **c** Alizarin Red S staining images of USSCs (objective magnification ×100) after 3 weeks of culture under osteogenic differentiation medium

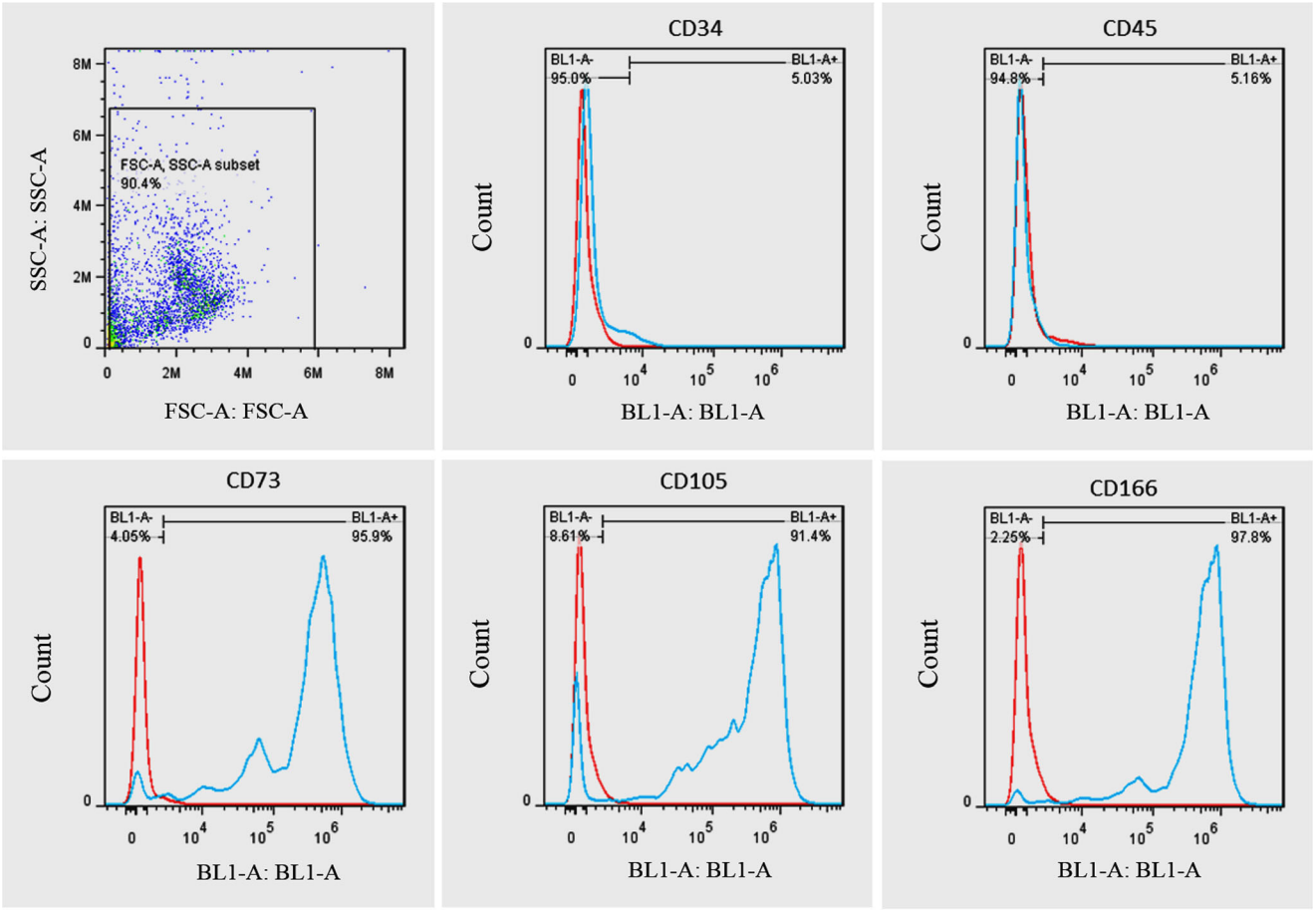

Fig. 5 Immunophenotyping of USSCs by flow cytometry. CD markers are shown in blue and the red line indicates background fluorescence. The results are presented as median (range)

standard of nerve bridging had a significantly higher rate of improvement compared to other groups at both time intervals (p value < 0.05). SFI values for this group were measured to be − 57.47 ± 7.51 and − 26. 67 ± 3.66 at the end of 4th and 8th week after surgery, respectively. NGCs containing USSCs had significantly greater SFI values compared to cell-free NGC group at 8th week post-surgery (− 53.6 ± 3.8 vs. − 64.7 ± 4.07, p value < 0.05). These results indicate that USSCs could exhibit better motor function recovery compared to cell-free NGCs.

Hot Plate Latency Time Analysis

HPL time test is used for sensory recovery measurement (Salehi et al. 2017). Figure 7 presents the data for the HPL time during the recovery period. Signs of recovery of nociceptive function were seen at 14 weeks after injury. The autograft group exhibited a significantly (p value < 0.05) better sensory recovery among other groups. However, the normal value of 4 s was unachievable (Hu et al. 1997). There was a significant

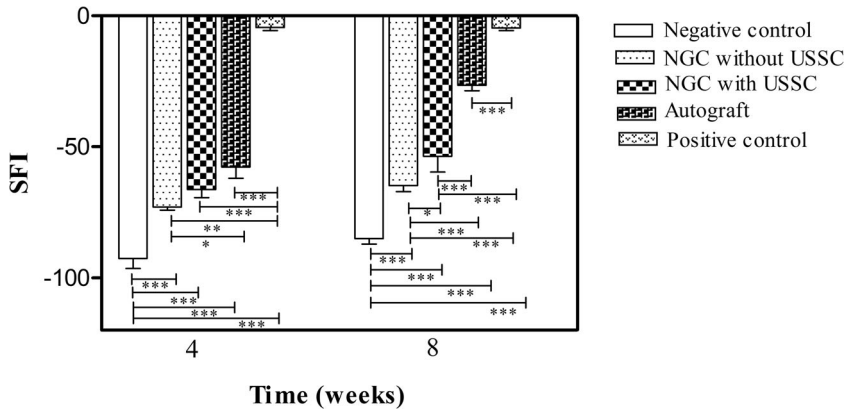

Fig. 6 Histogram comparing sciatic functional index study results of different groups 4 and 8 weeks post-surgery. Values represent the mean ± SD, $n = 4$, *$p < 0.05$, **$p < 0.01$, and ***$p < 0.005$

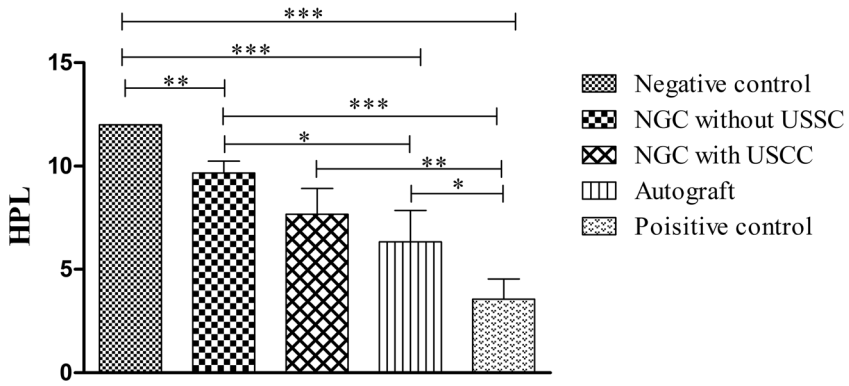

Fig. 7 Hot plate latency time measurement results 14 weeks post-surgery. Values represent the mean ± SD, $n = 4$, $*p < 0.05$, $**p < 0.01$, and $***p < 0.005$

difference between HPL time of rats treated with USSC containing NGCs and NGCs without cells (6.66 ± .96 s vs. 9.66 ± .57 s, p value < 0.05). This enhanced sensitivity to heat in the cell-containing NGC groups indicates that USSCs could possibly induce greater sensory axons regeneration.

Electrophysiological Studies

For electrophysiological assessment, the amplitude of CMAP indirectly reflects the motor nerves regeneration (Farzamfar et al. 2018). Measurements of peak amplitude (Fig. 8) showed that sciatic nerve of rats bridged with autograft nerve had the highest CMAP amplitude among all operated animals (representative EMG waveform images for different groups are shown in Fig. 9). These value for nerves bridged with USSC containing NGCs was nearest to the autograft group. The amplitude of CMAP in USSC delivering conduits was significantly higher than cell-free NGCs (22.4 ± 3.77 vs. 16.66 ± 2.08 mV, p value < 0.05). It can be inferred that USSCs could aid in re-innervating the damaged limb.

Gastrocnemius Muscle Wet Weight Loss

When the gastrocnemius muscle is denervated as a consequence of sciatic nerve injury, it undergoes atrophy and weight loss (Wu et al. 2015). The wet weight loss of the gastrocnemius muscle is a useful method to investigate the efficacy of muscle re-innervation. The lower the gastrocnemius muscle wet weight loss percentage, the better re-innervation of the muscle (Wang et al. 2014; Farzamfar et al. 2017). Figure 10

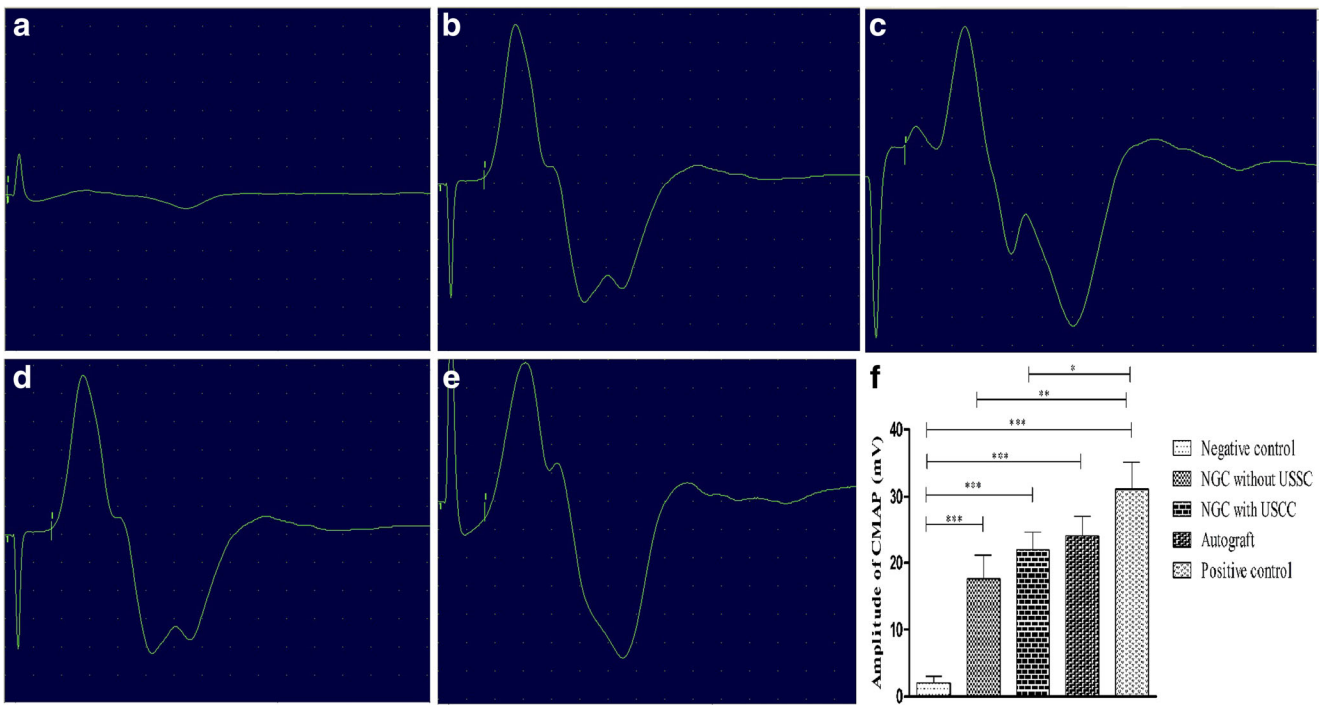

Fig. 8 Representative EMG waveform images for different groups. **a** EMG waveform image for Negative control, **b** for NGCs without USSCs, **c** for NGCs with USSCs, **d** for autograft, and **e** for the positive control group, **f** histogram comparing the amplitudes of compound muscle action potential 14 weeks after surgery. Values represent the mean ± SD, $n = 4$, $*p < 0.05$, $**p < 0.01$, and $***p < 0.005$

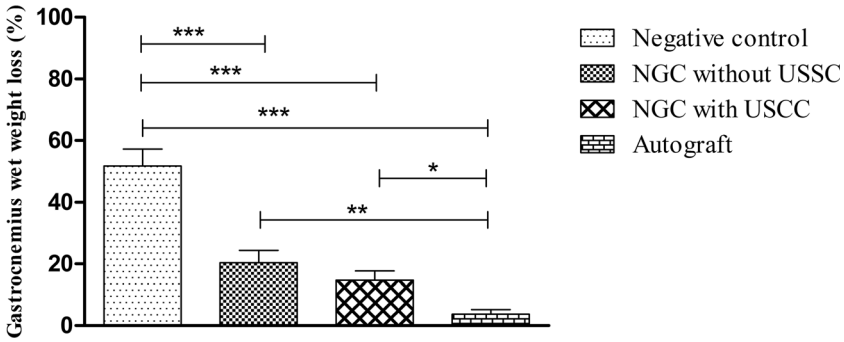

Fig. 9 Gastrocnemius muscle wet weight loss percentages of different groups after 14 weeks of surgery. Values represent the mean ± SD, $n = 4$, $*p < 0.05$, $**p < 0.01$, and $***p < 0.005$

shows that the autograft group had significantly smaller gastrocnemius muscle wet weight loss percentage compared to other groups (p value < 0.05). The weight loss percentage in the conduits containing USSCs was smaller than the NGCs without USSCs; however, the observed difference was not statistically significant.

Histopathological Assessments

After 14 weeks, the animals were sacrificed and the sciatic nerve and gastrocnemius muscle tissues were harvested for histopathological examinations. No signs of hematoma or infection were observed at the implantation site, indicating good tissue compatibility of the conduits which is in accordance with the MTT results. Figure 10 illustrates the histopathological examination of the sciatic nerves of all groups. Histopathological analysis of sciatic nerves showed that in the positive control group nerve fibers had well-arranged structure without any sign of damage. Nerve fibers were irregularly distributed in the negative control group. Axonal degeneration, perineural fibrosis, noticeable edema, and various degrees of vacuola formation were also clear in this group. In the autograft group, less axonal swelling and vacuolation were observed compared to the negative control group. Moreover, nerve fibers almost recovered their normal structure demonstrating improved fiber arrangement. Histopathological assessment of sciatic nerves bridged with NGCs without cells exhibited a mild myelin vacuolation and edema around nerve fibers. Histological evaluation of NGCs with USSCs group exhibited a considerable degree of regeneration compared to cell-free NGC group. NGC containing USSCs could partly alleviate the signs of nerve damage. Well-arranged nerve fibers, intact myelin sheath, and a negligible vacuolation and edema were evident in this group. Micrographs of muscle fibers (Fig. 10) in normal groups (positive control) showed that muscle fibers were intact with no sign of muscular atrophy. In the negative control group, cell connections were weak and muscular atrophy was evident. Fibrosis has dramatically increased between muscle bundles and the overall arrangement of the fibers was distorted. In the autograft group, the cell connections were relatively tight and the muscle could partly retain its normal structure. In the NGC without USSC group, a significantly lower degree of muscular fibers atrophy and fibrosis was observed when compared to the negative control group. In the NGC with USSC group, gastrocnemius muscle has recovered its normal structure and there was no evidence of fibrosis between the muscle bundles; however, mild atrophy was still seen in some fibers. In overall, the muscle bundles in the limbs treated with NGC + USSCs were more similar to those of the autograft group. Measuring the muscular area of the gastrocnemius muscle cross-sections by image pro-plus software (version 6.0, Media Cybernetics, Rockville, USA) showed that the cross-sectional area (Table 2) of the muscle bundles was the greatest in the normal muscles. In addition, this area was greater in the autograft group than NGC + USSC group and significantly greater in cell-laden NGCs compared to NGC without USSCs and in the negative control group (p value < 0.05).

Discussion

Peripheral nerve regeneration is a complex process of interrelated phases which is characterized by Wallerian degeneration, axonal sprouting, and re-myelination (Jiang et al. 2017). The accumulating body of evidences support the integral role of SCs in nerve regeneration (Frostick et al. 1998; Mosahebi et al. 2002). Despite showing promising results, harvest and expansion of SCs is time-consuming and requires the sacrifice of an autologous nerve with the accompanying complications (Dai et al. 2013; Wang et al. 2017). Therefore searching for alternative sources seems crucial.

This is the first study demonstrating the regenerative potential of USSCs for peripheral nerve regeneration. Our findings proved that USSCs delivered through a nanofibrous NGC had superior regenerative capacity compared to the same NGCs but without USSCs, as evidenced by an enhanced motor and sensory function recovery and histopathological examinations.

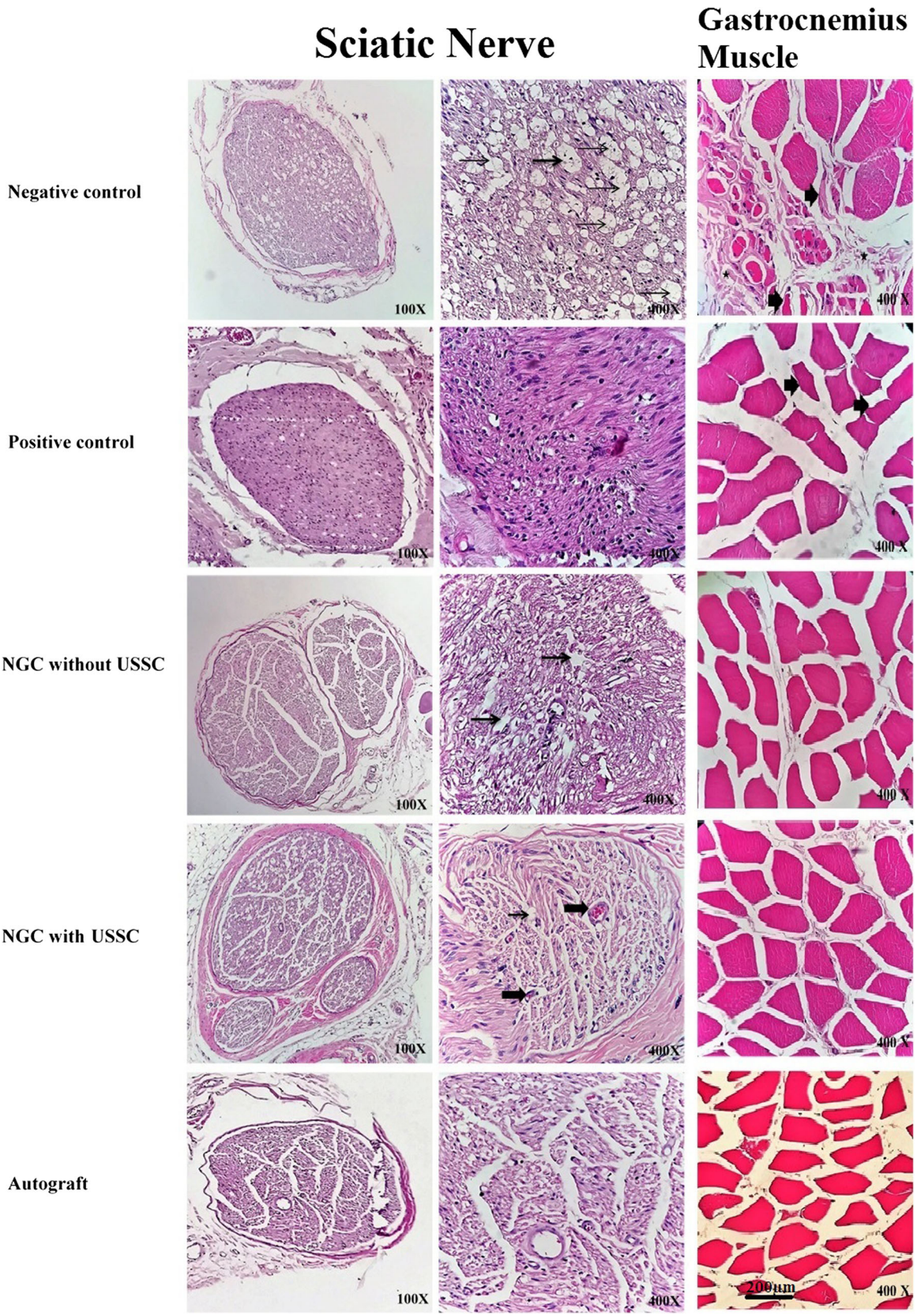

Fig. 10 Hematoxylin-eosin (H&E) stained images of the sciatic nerve and gastrocnemius muscle at the end of 14th-week post-surgery. Thin arrows and thick arrows indicate vacuolation and blood vessels respectively in the images of sciatic nerve. Thick arrows and asterisk indicate atrophied myocytes and fibrosis respectively in the image of gastrocnemius muscle

Table 2 The cross-sectional area (CSA) of the muscle bundles in different groups. Values represent the mean ± SD, $n = 4$, $^{*}p < 0.05$, $^{**}p < 0.01$, and $^{***}p < 0.005$. p value indicates treatment group versus negative control group

Groups	CSA
Negative control	821 ± 23
Positive control	1995 ± 66**
NGC without USSC	1222 ± 21*
NGC with USSC	1879 ± 41**
Autograft	1907 ± 67**

It has been shown that USSCs obtained from human umbilical cord blood has tri-lineage differentiation potential. Neural lineage differentiation capability of USSCs has been reported in vitro and in vivo (Kögler et al. 2004). Greschat et al. could show that under defined growth and differentiation factors incubation, USSCs acquired a neuronal phenotype and function (Greschat et al. 2008). Furthermore, Dastjerdi et al. showed that Wnt/β-catenin signaling pathway is involved in USSCs differentiation towards neural fate (Dastjerdi et al. 2012). Hence, the therapeutic potential of USSCs in sciatic nerve regeneration may be partly due to the inherent ability of USSCs to replace damaged neurons.

Neuroprotection capability of cord blood-derived stem cells has been proved by previous studies (Arien-Zakay et al. 2011; Lv et al. 2016). The mechanism by which stem cells exert their therapeutic effects is thought to be due to shuttling biological information and releasing soluble bioactive molecules (Andaloussi et al. 2013; Rani et al. 2015). Although less data is available with regard to USSCs secretion profile, it would be expected that USSCs may also secrete various neurotrophic factors which would have therapeutic benefits in peripheral nerve regeneration. Finally, USSCs seeded in the NGC may aid in regeneration by releasing extracellular matrix proteins that build up a basement membrane to provide a permissive environment for nerve repair (Jiang et al. 2017; Sullivan et al. 2016; Shirzadeh et al. 2018).

USSCs can be harvested in advance, expanded to clinically sufficient numbers, and cryopreserved until the time of transplantation. In addition to high differentiation potential of USSCs, they have a high proliferative activity which can be expanded in vitro without developing genetic abnormalities (Schira et al. 2015; Liao et al. 2014). On the other hand, the application of USSCS to repair nerve gaps may be associated with some complications that need to be addressed before any clinical trial. The clearest obstacle is cell survival after thawing and administration in the damaged site. The hostile environment in the injured tissue may also endanger cell viability (Amer et al. 2017; Tabar and Studer 2014). Another concern is that USSCs may differentiate into non-neural cell types. There is always the possibility that USSCs may differentiate into non-desired cell lineages (Ikehara 2013; Bongso et al. 2008). Therefore, strict regulations with adequate follow-ups must be taken into account to ensure the safety of the proposed treatment modality.

Conclusion

In the current study, USSCs delivered through a nanofibrous NGC could promote nerve regeneration over a 10-mm nerve gap with the comparable regenerative capacity to autograft group. Further studies need to be performed to follow-up long-term potential adverse effects of this cell type application in peripheral nerve regeneration. This preliminary study suggests that the USSCs can be used as a potential source for cell-based therapies in peripheral nerve injuries.

Acknowledgment The present study was supported by Shahroud University of medical sciences. We hereby acknowledge the research deputy for grant No 97130138.

Availability of Data and Material Not applicable.

Authors' Contributions All authors read and approved the final manuscript.

Compliance with Ethical Standards

Ethics Approval and Consent to Participate Animal experiments were approved by the ethics committee of the Shahroud University of Medical Sciences and were carried out in accordance with the university's guidelines.

Consent for Publication Not applicable.

Competing Interests The authors declare that they have no competing interests.

References

Ahmadbeigi N, Seyedjafari E, Gheisari Y, Atashi A, Omidkhoda A, Soleimani M (2010) Surface expression of CXCR4 in unrestricted somatic stem cells and its regulation by growth factors. Cell Biol Int 34(7):687–692

Alberts B, et al (2002) The extracellular matrix of animals.

Amer MH, Rose FRAJ, Shakesheff KM, Modo M, White LJ (2017) Translational considerations in injectable cell-based therapeutics for neurological applications: concepts, progress and challenges. NPJ Regen Med 2(1):23

Andaloussi SE et al (2013) Extracellular vesicles: biology and emerging therapeutic opportunities. Nat Rev Drug Discov 12(5):347–357

Arien-Zakay H, Lecht S, Nagler A, Lazarovici P (2011) Neuroprotection by human umbilical cord blood-derived progenitors in ischemic brain injuries. Arch Ital Biol 149(2):233–245

Barnes CP, Sell SA, Boland ED, Simpson DG, Bowlin GL (2007) Nanofiber technology: designing the next generation of tissue engineering scaffolds. Adv Drug Deliv Rev 59(14):1413–1433

Bhattarai N, Li Z, Gunn J, Leung M, Cooper A, Edmondson D, Veiseh O, Chen MH, Zhang Y, Ellenbogen RG, Zhang M (2009) Natural-synthetic polyblend nanofibers for biomedical applications. Adv Mater 21(27):2792–2797

Binulal N et al (2014) PCL–gelatin composite nanofibers electrospun using diluted acetic acid–ethyl acetate solvent system for stem cell-based bone tissue engineering. J Biomater Sci Polym Ed 25(4):325–340

Bongso A, Fong CY, Gauthaman K (2008) Taking stem cells to the clinic: major challenges. J Cell Biochem 105(6):1352–1360

Cao H, Liu T, Chew SY (2009) The application of nanofibrous scaffolds in neural tissue engineering. Adv Drug Deliv Rev 61(12):1055–1064

Chang H-I, Wang Y (2011) Cell responses to surface and architecture of tissue engineering scaffolds, In Regenerative medicine and tissue engineering-cells and biomaterials. INTECH

Dai L-G, Huang G-S, Hsu S-h (2013) Sciatic nerve regeneration by cocultured Schwann cells and stem cells on microporous nerve conduits. Cell Transplant 22(11):2029–2039

Dastjerdi FV, Zeynali B, Tafreshi AP, Shahraz A, Chavoshi MS, Najafabadi IK, Vardanjani MM, Atashi A, Soleimani M (2012) Inhibition of GSK-3β enhances neural differentiation in unrestricted somatic stem cells. Cell Biol Int 36(11):967–972

de Ruiter GC et al (2009) Designing ideal conduits for peripheral nerve repair. Neurosurg Focus 26(2):E5

di Summa PG, Kingham PJ, Raffoul W, Wiberg M, Terenghi G, Kalbermatten DF (2010) Adipose-derived stem cells enhance peripheral nerve regeneration. J Plast Reconstr Aesthet Surg 63(9):1544–1552

Fairbairn NG, Meppelink AM, Ng-Glazier J, Randolph MA, Winograd JM (2015) Augmenting peripheral nerve regeneration using stem cells: a review of current opinion. World J Stem Cells 7(1):11–26

Faroni A et al (2015) Peripheral nerve regeneration: experimental strategies and future perspectives. Adv Drug Deliv Rev 82:160–167

Farzamfar S, Naseri-Nosar M, Ghanavatinejad A, Vaez A, Zarnani AH, Salehi M (2017) Sciatic nerve regeneration by transplantation of menstrual blood-derived stem cells. Mol Biol Rep 44(5):407–412

Farzamfar S, Naseri-Nosar M, Vaez A, Esmaeilpour F, Ehterami A, Sahrapeyma H, Samadian H, Hamidieh AA, Ghorbani S, Goodarzi A, Azimi A, Salehi M (2018) Neural tissue regeneration by a gabapentin-loaded cellulose acetate/gelatin wet-electrospun scaffold. Cellulose 25(2):1229–1238

Fauza DO, Bani M (eds) (2016) Fetal stem cells in regenerative medicine: Principles and translational strategies. Springer, 2016

Frostick SP, Yin Q, Kemp GJ (1998) Schwann cells, neurotrophic factors, and peripheral nerve regeneration. Microsurgery 18(7):397–405

Fu W et al (2014) Electrospun gelatin/PCL and collagen/PLCL scaffolds for vascular tissue engineering. Int J Nanomedicine 9:2335

Gao M, Lu P, Lynam D, Bednark B, Campana WM, Sakamoto J, Tuszynski M (2016) BDNF gene delivery within and beyond templated agarose multi-channel guidance scaffolds enhances peripheral nerve regeneration. J Neural Eng 13(6):066011

Gautam S, Dinda AK, Mishra NC (2013) Fabrication and characterization of PCL/gelatin composite nanofibrous scaffold for tissue engineering applications by electrospinning method. Mater Sci Eng C 33(3):1228–1235

Ghasemi-Mobarakeh L, Semnani D, Morshed M (2007) A novel method for porosity measurement of various surface layers of nanofibers mat using image analysis for tissue engineering applications. J Appl Polym Sci 106(4):2536–2542

Ghasemi-Mobarakeh L, Prabhakaran MP, Morshed M, Nasr-Esfahani MH, Ramakrishna S (2008) Electrospun poly (ε-caprolactone)/gelatin nanofibrous scaffolds for nerve tissue engineering. Biomaterials 29(34):4532–4539

Ghodsizad A, Niehaus M, Kögler G, Martin U, Wernet P, Bara C, Khaladj N, Loos A, Makoui M, Thiele J, Mengel M, Karck M, Klein HM, Haverich A, Ruhparwar A (2009) Transplanted human cord blood-derived unrestricted somatic stem cells improve left-ventricular function and prevent left-ventricular dilation and scar formation after acute myocardial infarction. Heart 95(1):27–35

Greschat S, Schira J, Küry P, Rosenbaum C, de Souza Silva MA, Kögler G, Wernet P, Müller HW (2008) Unrestricted somatic stem cells from human umbilical cord blood can be differentiated into neurons with a dopaminergic phenotype. Stem Cells Dev 17(2):221–232

Hoque ME et al (2015) Gelatin based scaffolds for tissue engineering—a review. Polymers Res J 9(1):15

Hu D, Hu R, Berde CB (1997) Neurologic evaluation of infant and adult rats before and after sciatic nerve blockade. Anesthesiology 86(4):957–965

Huang Z-M, Zhang YZ, Ramakrishna S, Lim CT (2004) Electrospinning and mechanical characterization of gelatin nanofibers. Polymer 45(15):5361–5368

Ikehara S (2013) Grand challenges in stem cell treatments. Front Cell Dev Biol 1:2

Jessen K, Mirsky R (2016) The repair Schwann cell and its function in regenerating nerves. J Physiol 594(13):3521–3531

Jessen KR, Mirsky R, Lloyd AC (2015) Schwann cells: development and role in nerve repair. Cold Spring Harb Perspect Biol 7(7):a020487

Jiang X, Mi R, Hoke A, Chew SY (2014) Nanofibrous nerve conduit-enhanced peripheral nerve regeneration. J Tissue Eng Regen Med 8(5):377–385

Jiang L, Jones S, Jia X (2017) Stem cell transplantation for peripheral nerve regeneration: current options and opportunities. Int J Mol Sci 18(1):94

Kehoe S, Zhang X, Boyd D (2012) FDA approved guidance conduits and wraps for peripheral nerve injury: a review of materials and efficacy. Injury 43(5):553–572

Kemp SW, Walsh SK, Midha R (2008) Growth factor and stem cell enhanced conduits in peripheral nerve regeneration and repair. Neurol Res 30(10):1030–1038

Kögler G, Sensken S, Airey JA, Trapp T, Müschen M, Feldhahn N, Liedtke S, Sorg RV, Fischer J, Rosenbaum C, Greschat S, Knipper A, Bender J, Degistirici Ö, Gao J, Caplan AI, Colletti EJ, Almeida-Porada G, Müller HW, Zanjani E, Wernet P (2004) A new human somatic stem cell from placental cord blood with intrinsic pluripotent differentiation potential. J Exp Med 200(2):123–135

Kweon H, Yoo MK, Park IK, Kim TH, Lee HC, Lee HS, Oh JS, Akaike T, Cho CS (2003) A novel degradable polycaprolactone networks for tissue engineering. Biomaterials 24(5):801–808

Lannutti J, Reneker D, Ma T, Tomasko D, Farson D (2007) Electrospinning for tissue engineering scaffolds. Mater Sci Eng C 27(3):504–509

Lee B-K, Ju YM, Cho JG, Jackson JD, Lee SJ, Atala A, Yoo JJ (2012) End-to-side neurorrhaphy using an electrospun PCL/collagen nerve conduit for complex peripheral motor nerve regeneration. Biomaterials 33(35):9027–9036

Lee J-Y, Giusti G, Wang H, Friedrich PF, Bishop AT, Shin AY (2013) Functional evaluation in the rat sciatic nerve defect model: a comparison of the sciatic functional index, ankle angles, and isometric tetanic force. Plast Reconstr Surg 132(5):1173–1180

Li C, Vepari C, Jin HJ, Kim HJ, Kaplan DL (2006) Electrospun silk-BMP-2 scaffolds for bone tissue engineering. Biomaterials 27(16):3115–3124

Liao Y, Itoh M, Yang A, Zhu H, Roberts S, Highet AM, Latshaw S, Mitchell K, van de Ven C, Christiano A, Cairo MS (2014) Human cord blood-derived unrestricted somatic stem cells promote wound healing and have therapeutic potential for patients with recessive dystrophic epidermolysis bullosa. Cell Transplant 23(3):303–317

Liu X, Smith LA, Hu J, Ma PX (2009) Biomimetic nanofibrous gelatin/apatite composite scaffolds for bone tissue engineering. Biomaterials 30(12):2252–2258

Luo L, Gan L, Liu Y, Tian W, Tong Z, Wang X, Huselstein C, Chen Y (2015) Construction of nerve guide conduits from cellulose/soy protein composite membranes combined with Schwann cells and pyrroloquinoline quinone for the repair of peripheral nerve defect. Biochem Biophys Res Commun 457(4):507–513

Lv XM et al (2016) Human umbilical cord blood-derived stem cells and brain-derived neurotrophic factor protect injured optic nerve: viscoelasticity characterization. Neural Regen Res **11**(4):652

Ma F, Zhu T, Xu F, Wang Z, Zheng Y, Tang Q, Chen L, Shen Y, Zhu J (2017) Neural stem/progenitor cells on collagen with anchored basic fibroblast growth factor as potential natural nerve conduits for facial nerve regeneration. Acta Biomater 50:188–197

Marín P (2016) Stem Cells and Regenerative Medicine. Handbook of translational medicine p. 109

Meng Z et al (2010) Electrospinning of PLGA/gelatin randomly-oriented and aligned nanofibers as potential scaffold in tissue engineering. Mater Sci Eng C 30(8):1204–1210

Miller C, Peek AL, Power D, Heneghan NR (2017) Psychological consequences of traumatic upper limb peripheral nerve injury: A systematic review. Hand Therapy 22(1):35–45

Mimeault M, Hauke R, Batra S (2007) Stem cells: a revolution in therapeutics—recent advances in stem cell biology and their therapeutic applications in regenerative medicine and cancer therapies. Clin Pharmacol Ther 82(3):252–264

Mosahebi A, Fuller P, Wiberg M, Terenghi G (2002) Effect of allogeneic Schwann cell transplantation on peripheral nerve regeneration. Exp Neurol 173(2):213–223

Muheremu A, Ao Q (2015) Past, present, and future of nerve conduits in the treatment of peripheral nerve injury. Biomed Res Int 2015:1–6

Murakami S, Kitamura M, Yamada S, Takedachi M (2016) Emerging regenerative approaches for periodontal regeneration: from cytokine therapy to stem-cell therapy. Curr Issues Periodontics 5

Naseri-Nosar M, Farzamfar S, Sahrapeyma H, Ghorbani S, Bastami F, Vaez A, Salehi M (2017) Cerium oxide nanoparticle-containing poly (ε-caprolactone)/gelatin electrospun film as a potential wound dressing material: in vitro and in vivo evaluation. Mater Sci Eng C 81: 366–372

Nauta AJ, Fibbe WE (2007) Immunomodulatory properties of mesenchymal stromal cells. Blood 110(10):3499–3506

Parenteau-Bareil R, Gauvin R, Berthod F (2010) Collagen-based biomaterials for tissue engineering applications. Materials 3(3):1863–1887

Peng S, Jin G, Li L, Li K, Srinivasan M, Ramakrishna S, Chen J (2016) Multi-functional electrospun nanofibres for advances in tissue regeneration, energy conversion & storage, and water treatment. Chem Soc Rev 45(5):1225–1241

Polymeri A, Giannobile W, Kaigler D (2016) Bone marrow stromal stem cells in tissue engineering and regenerative medicine. Horm Metab Res 48(11):700–713

Rani S, Ryan AE, Griffin MD, Ritter T (2015) Mesenchymal stem cell-derived extracellular vesicles: toward cell-free therapeutic applications. Mol Ther 23(5):812–823

Salehi M, Naseri Nosar M, Amani A, Azami M, Tavakol S, Ghanbari H (2015) Preparation of pure PLLA, pure chitosan, and PLLA/chitosan blend porous tissue engineering scaffolds by thermally induced phase separation method and evaluation of the corresponding mechanical and biological properties. Int J Polym Mater Polym Biomater 64(13):675–682

Salehi M, Naseri-Nosar M, Ebrahimi-Barough S, Nourani M, Khojasteh A, Hamidieh AA et al (2017) Sciatic nerve regeneration by transplantation of Schwann cells via erythropoietin controlled-releasing polylactic acid/multiwalled carbon nanotubes/gelatin nanofibrils neural guidance conduit. J Biomater Mater Res B Appl Biomater

Sanen K, Martens W, Georgiou M, Ameloot M, Lambrichts I, Phillips J (2017) Engineered neural tissue with Schwann cell differentiated human dental pulp stem cells: potential for peripheral nerve repair? J Tissue Eng Regen Med 11(12):3362–3372

Santourlidis S, Wernet P, Ghanjati F, Graffmann N, Springer J, Kriegs C, Zhao X, Brands J, Araúzo-Bravo MJ, Neves R, Koegler G, Uhrberg M (2011) Unrestricted somatic stem cells (USSC) from human umbilical cord blood display uncommitted epigenetic signatures of the major stem cell pluripotency genes. Stem Cell Res 6(1):60–69

Sarasam A, Madihally SV (2005) Characterization of chitosan–polycaprolactone blends for tissue engineering applications. Biomaterials 26(27):5500–5508

Schira J, Falkenberg H, Hendricks M, Waldera-Lupa DM, Kögler G, Meyer HE, Müller HW, Stühler K (2015) Characterization of regenerative phenotype of unrestricted somatic stem cells (USSC) from human umbilical cord blood (hUCB) by functional secretome analysis. Mol Cell Proteomics 14(10):2630–2643

Schwartz PH et al (2008) Differentiation of neural lineage cells from human pluripotent stem cells. Methods 45(2):142–158

Shirzadeh E, Heidari Keshel S, Ezzatizadeh V, Jabbehdari S, Baradaran-Rafii A (2018) Unrestricted somatic stem cells, as a novel feeder layer: ex vivo culture of human limbal stem cells. J Cell Biochem 119(3):2666–2678

Sill TJ, von Recum HA (2008) Electrospinning: applications in drug delivery and tissue engineering. Biomaterials 29(13):1989–2006

Sparling JS, Bretzner F, Biernaskie J, Assinck P, Jiang Y, Arisato H, Plunet WT, Borisoff J, Liu J, Miller FD, Tetzlaff W (2015) Schwann cells generated from neonatal skin-derived precursors or neonatal peripheral nerve improve functional recovery after acute transplantation into the partially injured cervical spinal cord of the rat. J Neurosci 35(17):6714–6730

Sullivan R, Dailey T, Duncan K, Abel N, Borlongan C (2016) Peripheral nerve injury: stem cell therapy and peripheral nerve transfer. Int J Mol Sci 17(12):2101

Tabar V, Studer L (2014) Pluripotent stem cells in regenerative medicine: challenges and recent progress. Nat Rev Genet 15(2):82–92

Tran PA, Hocking DM, O'Connor AJ (2015) In situ formation of antimicrobial silver nanoparticles and the impregnation of hydrophobic polycaprolactone matrix for antimicrobial medical device applications. Mater Sci Eng C 47:63–69

Tung W, Tam K, Chan Y, Shum D (eds) (2015) Nerve conduit constructed by aligned chitosan nanofibers for directing axonal growth in nerve regeneration. International Symposium on Healthy Aging

Wang S, Yaszemski MJ, Knight AM, Gruetzmacher JA, Windebank AJ, Lu L (2009) Photo-crosslinked poly (ε-caprolactone fumarate) networks for guided peripheral nerve regeneration: material properties and preliminary biological evaluations. Acta Biomater 5(5):1531–1542

Wang W et al (2014) Craniocerebral injury promotes the repair of peripheral nerve injury. Neural Regen Res 9(18):1703–1708

Wang G, Cao L, Wang Y, Hua Y, Cai Z, Chen J, Chen L, Jin Y, Niu L, Shen H, Lu Y, Shen Z (2017) Human eyelid adipose tissue-derived Schwann cells promote regeneration of a transected sciatic nerve. Sci Rep 7:43248

Wu R, Yan Y, Yao J, Liu Y, Zhao J, Liu M (2015) Calpain 3 expression pattern during gastrocnemius muscle atrophy and regeneration following sciatic nerve injury in rats. Int J Mol Sci 16(11):26927–26935

Xie J, MacEwan MR, Schwartz AG, Xia Y (2010) Electrospun nanofibers for neural tissue engineering. Nanoscale 2(1):35–44

Xie J, Liu W, MacEwan MR, Bridgman PC, Xia Y (2014) Neurite outgrowth on electrospun nanofibers with uniaxial alignment: the effects of fiber density, surface coating, and supporting substrate. ACS Nano 8(2):1878–1885

Yao R, He J, Meng G, Jiang B, Wu F (2016) Electrospun PCL/gelatin composite fibrous scaffolds: mechanical properties and cellular responses. J Biomater Sci Polym Ed 27(9):824–838

Zhang Y et al (2005) Electrospinning of gelatin fibers and gelatin/PCL composite fibrous scaffolds. J Biomed Mater Res B Appl Biomater 72(1):156–165